A deformation analysis of a dynamic estuary using two-weekly MBES surveying

Steven Pluymaekers, Roderik Lindenbergh and Dick Simons
Delft Institute of Earth Observation and Space Systems,
Delft University of Technology,
P.O. Box 5058, 2600 GB Delft,
The Netherlands.
Email: r.c.lindenbergh@tudelft.nl

John de Ronde
RIKZ, Dutch National Institute of
Coastal and Marine Management,
P.O. Box 20907, 2500 EX The Hague,
The Netherlands.
Email: J.G.dRonde@rikz.rws.minvenw.nl

***Abstract*—A method is introduced and tested to analyze changes in depth and subaqueous dune parameter values in the complex topography of a multichannel estuary system. Periodic bedforms as represented by Multibeam Echo Sounding (MBES) data are first separated from the raw topography in a filtering procedure. Then dune parameter class maps are determined from the bedform component of the data. These division in classes enables a segmentation of the area in regions of similar morphological behavior. The method is demonstrated on a time series of 17 two-weekly MBES data sets representing the estuary floor near Walsoorden in the Western Scheldt estuary. Two areas are analyzed in detail: a sand dump and its direct neighborhood and a more stable area, selected by the segmentation procedure.**

I. Introduction

In the so-called Long Term Vision program the governments of Belgium and The Netherlands are working together on a long term strategy for the management of the Scheldt estuary, containing in particular the Western Scheldt river delta. This estuary system, while situated in The Netherlands, connects the North Sea to the main Belgium harbor, that of Antwerp. Part of this program is the case study Walsoorden, [1]. The ministry of the Vlaamse gemeenschap is performing a morphological monitoring program of a test sand dump near Walsoorden in the Western Scheldt. The monitoring program has resulted in a time series of Multibeam Echo Sounding (MBES) data. The special thing about this time series of seventeen epochs is the short interval between the consecutive moments of sounding: during and after the sand dump, the Western Scheldt bottom was monitored at a two week interval.

This unique data set allows us to address the following questions:

- How does the sand dump change over time? Is it eroding and if so, is it possible to find the sand back elsewhere in the area? How fast are bed-forms reappearing on top of the sand dump and how do their parameter values, like sand wavelength and amplitude evolve?
- How does a parameter value map of morphological parameters like channel location, sand wave amplitude and length or sand wave orientation look like and how are these parameter values changing over time?
- The exact sounding data are known. Therefore it is possible to find out the weather conditions in between the soundings from easily available meteorological data. Is there a relation between changes in the morphological parameter values and the weather condition?

Answers to these questions are found by combining several techniques. Signal decomposition is performed to separate large scale topography from different scales of bed-forms, [2], to obtain a more reliable parameter value estimation. A segmentation step is proposed to distinguish between different deformation regimes at locations with different characteristics in topography and bed-form parameters, while deformation in homogeneous areas is traced by applying the Delft method, [3], of deformation analysis, which compares different deformation scenarios in a data snooping procedure, while incorporating the uncertainty and correlation in the input data. Using this combination of techniques provides a way of ordering the complex morpho-dynamics in the Western Scheldt double-channel system from a data point of view.

In Section II the area and the MBES data representing it are introduced, in Section III an overview is given of the used methodology, while the results of the morpho-dynamic analysis are given in Section IV. The paper finishes with conclusions.

II. Area and Data description

The Western Scheldt is located in the South-West of The Netherlands, see Fig. 1. It is the most seaward part of the estuary of the Scheldt river and it constitutes the connection between the North-Sea on the West and the harbor of Antwerpen, just over the border with Belgium, in the East. The Scheldt estuary is an example of a dynamic meandering ebb-flood channel system, [4], [5], that is, it consist of tidal channels, separated by elongated tidal flats and flanked by salt marshes. These morphological features form a unique ecosystem, [6], therefore one important focus of management scenarios is on maintaining this system. The other main focus is on maintaining access to the Antwerpen harbor on a scale that keeps up with current economic standards, implying a continuous increase in draught of passing vessels. Guaranteeing Antwerpen harbor access means that a critical depth in

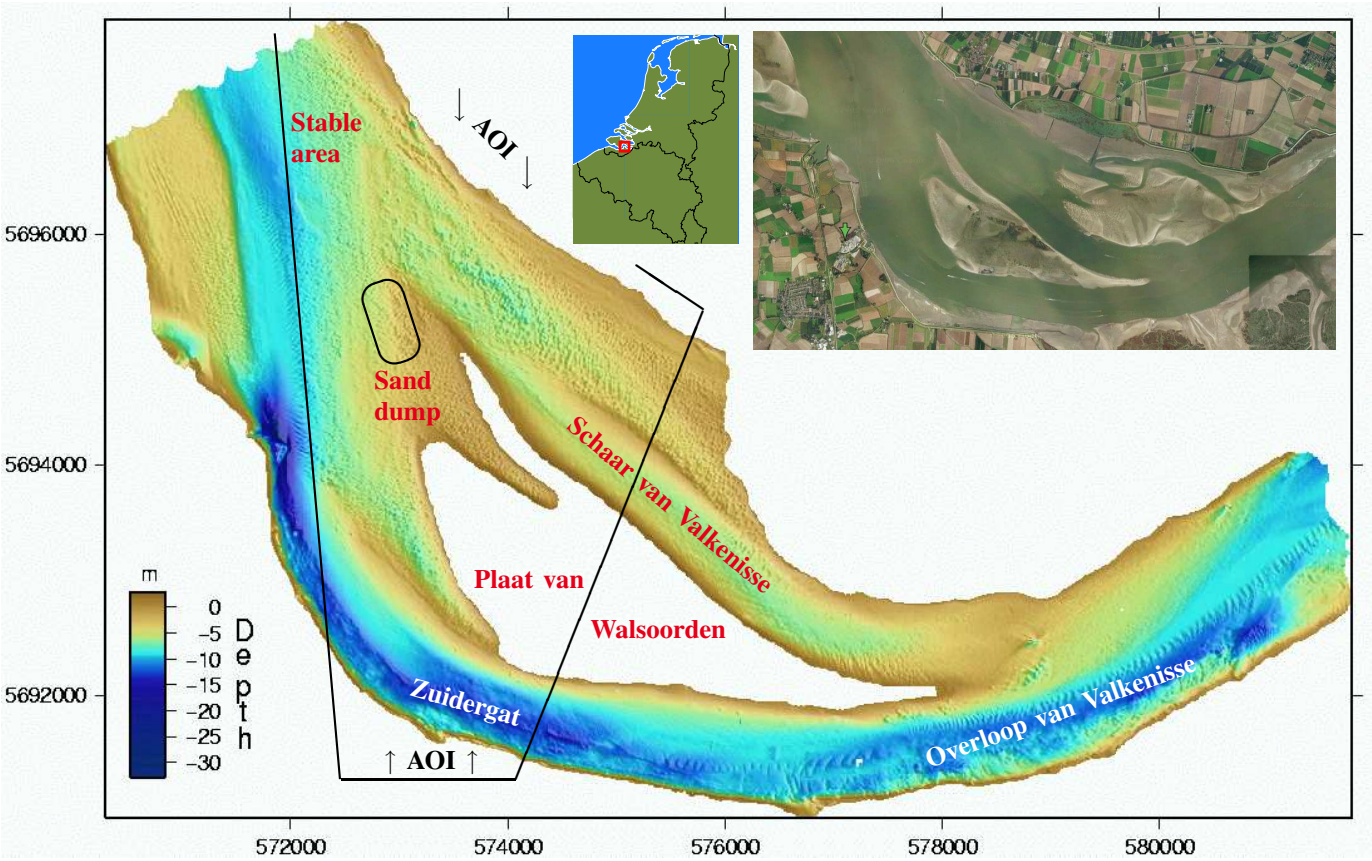

Fig. 1. Overview Walsoorden MBES data set. Large inset: areal photo Walsoorden area. Small inset: location Walsoorden.

the tidal channels has to be enforced by dredging. To reduce dredging costs it is preferable to deposit the dredged material as close as possible to the dredging location.

These two points of attention leaded to the Walsoorden data set, [1]. In early winter 2004, a sand dump took place near the village of Walsoorden, see Fig. 1. The Walsoorden area roughly exists of a deep ebb channel in the South, het Zuidergat, separated by a tidal flat, the Plaat van Walsoorden, from a flood channel, the Schaar van Valkenisse. In the East, the two channels merge in the Overloop van Valkenisse, [5].

In order to assess the impact on the ecosystem and the shipping channels, the region was monitored by MBES, [7], at a two weeks interval, starting shortly before the dump. For this purpose the SIMRAD EM 3002 Dual head MBES was used. It must be mentioned that the dataset was interpolated on a rectangular 1 meter by 1 meter grid on forehand. The surveys used in this research cover and area of interest (AOI) that comprises basically the Western half of the visualized big data set, Fig. 1. The seventeen available data epochs are listed in Table I.

TABLE I
DATA EPOCHS, AREA OF INTEREST (AOI)

Survey	date	year	day
T0	07-11	2004	7
T1	23-11		23
T2	29-11		29
T3	13-12		43
T4	22-12		52
T5	10-01	2005	71
T6	25-01		86
T7	03-02		95
T8	09-02		101
T9	17-02		109
T10	24-02		116
T11	04-03		124
T12	10-03		130
T13	17-03		137
T14	11-04		162
T15	02-05		183
T16	23-05		204

III. METHODOLOGY

In this section methodology is described aiming at quantifying changes in estuary depth and suited bedform parameters. First these parameters are defined. Than it is described why and how to separate bedforms from the raw channel topography. Deformation regimes can be grouped by a segmentation strategy. After this pre-work finally a stochastic deformation analysis can be performed.

A. Bedform parameterization

The Scheldt estuary is covered by subaqueous dunes, [8], periodic bedforms of about 60 cm high with a wavelength in the order of 25 meter, caused by the flow of the water current over the sediment covering the estuary floor. In Fig. 1 some larger example are visible, e.g. in the Overloop van Valkenisse. Here, three parameters describing these bedforms are considered. The *amplitude* of a sand dune is defined as half the vertical distance between its highest and lowest point. The *orientation* of a dune field is the direction in clock wise direction from North in which maximal variation in depth occurs. The *wavelength* is the (average) horizontal distance, in the direction of the dune field orientation, between two consecutive dune crests (maxima) and troughs (minima).

B. Filtering

Processing of MBES data is strongly influenced by the presence of subaqueous dunes. Dunes and other periodic bedforms act as noise when assessing changes in global topography, e.g. for monitoring silting processes. Sand dune parameter estimation on the other hand will be biased in case of local changes in topography, at for example steep terrain. These problems can be solved by a signal decomposition step in which the global topography is separated from the bedforms. More sophisticated signal decomposition methods include signal approximation by means of Fourier polynomials or by geostatistical interpolation, [2]. Here a low pass filter is applied, [9]. Filtering a data set involves the creation of a moving window, the kernel, containing an array of weighting factors that is moved over the data. A new data value at the center of the kernel is obtained by multiplying each coefficient in the kernel with the corresponding data value in the kernel window. Performing this operation at each grid point creates a smoothed version of the original data set. The effect of the filter depends on the size of the kernel and the kernel coefficients.

C. Subaqueous dune parameter estimation.

After separating the underwater dunes from the large scale topography we proceed with estimating the above defined dune parameter values.

1) Dune orientation: The local sand dune orientation can be determined by a variability analysis, [10]. For this purpose variabilities in depth $(z_i - z_j)^2$ are computed for pairs of depth observations $x_i y_i z_i$ and $x_j y_j z_j$. The results are grouped with respect to the difference in length and direction of the positional difference vectors $(x_i - x_j, y_i - y_j)$. When averaging the results per difference class, the anisotropic, experimental variogram is obtained, [11]. Along the dune crests, the average variability will be minimal, the perpendicular direction gives the dune orientation. Examples of experimental directional variograms are given by the dotted lines in Fig. 2. A way to obtain a grid-point wise dune orientation is to draw profiles of equal length through a grid-point at regular angle intervals. The angle of the profile with the highest number of local extrema gives the dune orientation.

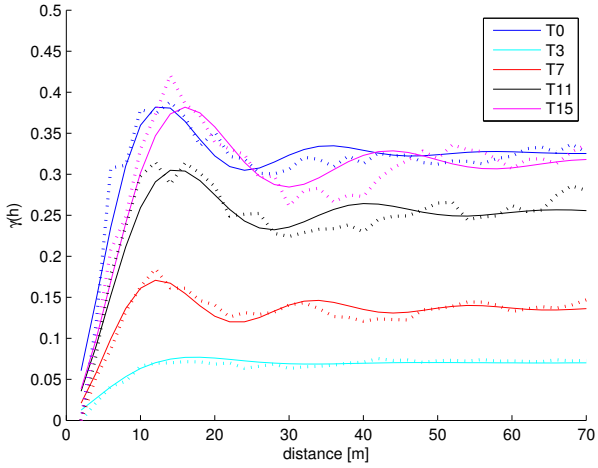

Fig. 2. Variograms in the dune orientation direction at the sand dump.

2) Dune amplitude and wavelength: Given the orientation of a subaqueous dune field, the average amplitude and wavelength is determined in two different ways. To the experimental directional variogram in the sand dune direction a hole-effect variogram model, [12], can be fitted. In such a model first the variability is increasing to a maximum value after which it drops to a local minimum, compare Fig. 2, where the model functions as fitted to the experimental variograms are given by the continuous lines. If such a model is fitted to an experimental variogram in the sand dune direction, the maximum variability is directly linked to the dune amplitude, while the range to the first local minimum indicates the dune wavelength. Alternatively, the dune amplitude and wavelength can be determined from the horizontal and vertical distances between trough and crest points in smoothed data profiles in the direction of the sand dune orientation.

D. Segmentation

The morphology of multichannel estuary systems is strongly varying with location. An example is shown in Fig. 3, an areal photograph of sand dunes on top of the Plaat van Walsoorden,

Fig. 3. Dunes on top of the Plaat van Walsoorden. [Source: Google maps]

compare Fig. 1. Apparently, the wavelength of these dunes completely changes over a distance of only 150 m. Different sand dune parameter values indicate different morphological processes. Therefore different results of a deformation analysis may be expected as well. Moreover, the previously described filtering step depends on the size and shape of the bedforms: to separate larger bedforms from a data set, a larger kernel size is needed. This demonstrates the need for spatially grouping of similar observations.

Here similarity is classified with respect to the attributes estuary depth, dune wavelength and dune amplitude. Other useful classification attributes include dune orientation or grain size. A first insight in the power of discernment of an additional attribute can be assessed by means of a principal component analysis, [9]: if an additional attribute is highly correlated with an attribute already in use, little classification power is gained by adding this extra attribute.

The strongly varying morphology causes problems in the classification process. The initial subdivision into suited classes results in noisy class maps: starting from a crest instead of from a trough may result in an (artificial) difference in wavelength class for example. Noisy class maps can be smoothened by morphological image processing operations, [13]. The basic operations are *dilation* and *erosion*. Both use a structural element or kernel, that is, a, not necessarily symmetric window of neighboring grid-points. Erosion is a shrinking operation. The structuring element is laid over the grid-point at hand and the attribute value is replaced by the lowest value within the element window. In the case of dilation the highest value is chosen. The closing operation, consisting of a dilation followed by an erosion using the same structural element, fills holes of size and shape depending on this element. The dune wavelength and amplitude class maps are generalized by a closing operation, followed by an erosion. Then small patches are removed and the final result is obtained from a majority operation in which a grid-point value is replaced by a value that occurs in the majority of the grid-points in a suited neighborhood.

E. Stochastic deformation analysis

The purpose of (stochastic) deformation analysis is to either select that mathematical model that describes best the changes in a time series of observations or to reject all available models. In both cases the individual quality of the observations is taken into account, by implementing the theory of adjustment and testing, [3], [14]. In adjustment theory a vector of observations $\underline{y}$ is adjusted to a, say, linear model A by solving the system

$$E\{\underline{y}\} \;=\; A \cdot \underline{x}; \qquad D\{\underline{y}\} \;=\; Q_y. \tag{1}$$

Here Q_y is the variance-covariance matrix of the observations, describing basically the individual quality of and the correlation between the observations. The solution of system 1 is given by the Best Linear Unbiased Estimator

$$\underline{\hat{x}} \;=\; (A^\top \cdot Q_y^{-1} \cdot A)^{-1} \cdot A^\top \cdot Q_y^{-1} \cdot \underline{y}. \tag{2}$$

A measure for the suitability of the A-model to describe the observations is given by the test statistic T_q, defined by

$$T_q \;=\; \underline{\hat{e}}^\top \cdot Q_y^{-1} \cdot \underline{\hat{e}} \tag{3}$$

with $\underline{\hat{e}} = A \cdot \underline{\hat{x}} - \underline{y}$ the vector of model residuals. In an overall model test this test statistic is compared to a suited critical value to decide whether it is likely, given the uncertainty in the observations, that the A-model is correct. Alternatively, it can be tested whether an extension of the A-model gives a significant improvement in adjustment.

In the case at hand the observation vector $\underline{y}$ consists of grid-point wise depth observations over time. Either original observations are used or observations from which the sand dune component is removed. A stable depth is described by the one parameter model $E\{y_{t_i}\} = d$, that is the depth d is constant and independent of the moment of sounding t_i. A constant upward or downward change is modeled by the two parameter model $E\{y_{t_i}\} = (1 \;\; t_i) \cdot (d_0 \;\; v)^\top$, with d_0 the initial depth and v the constant depth change. Using the testing procedure it can be decided if a grid-point should be considered stable, is eroding or silting at a constant rate or if none of these scenarios apply.

IV. Results

The methodology of Section III is applied in two different cases. First for the detection and analysis of the sand dump area, where strong changes are expected. Second, a homogeneous and probably more stable area is selected by means of the classification procedure. For both areas the development of the sand dune parameters over time is inspected. First the classification results for the whole area of interest are given based the first epoch, T0.

A. Classification results.

For all grid points in the area of interest, cf. Fig. 1, the sand dune orientation is determined by selecting that profile through the grid-point that has the largest number of local extrema. The values and locations of the local extrema are then used to obtain dune amplitude and wavelength. Based on the histograms of the obtained values, suited classes are defined. For the amplitude four classes are used: $\leq$ 30 cm, 30-40 cm, 40-50 cm, and $>$ 50 cm. For the wavelength the classes $\leq$ 16 m, 16-18 m, 18-21 m, and $>$ 21 m are defined. The initial amplitude and wavelength class maps are generalized by the morphological closing and majority operations, using structuring elements of 5 $\times$ 5 meter and 3 $\times$ 3 meter, resp. The final class maps are shown in Fig. 4, together with a map showing six depth classes ranging from 0 to 15 m.

Some corresponding segments can be pointed out: for example, the segment of small amplitudes in the South, Fig. 4.A, is very similar to a segment with small wavelengths, Fig. 4.C. It is also clear however from the classification maps, that no strong relation exists between the attributes dune amplitude, depth and dune wavelength. This observation is confirmed by the correlation values in Table II. A weak correlation of 0.41 exists between amplitude and wavelength, but almost no

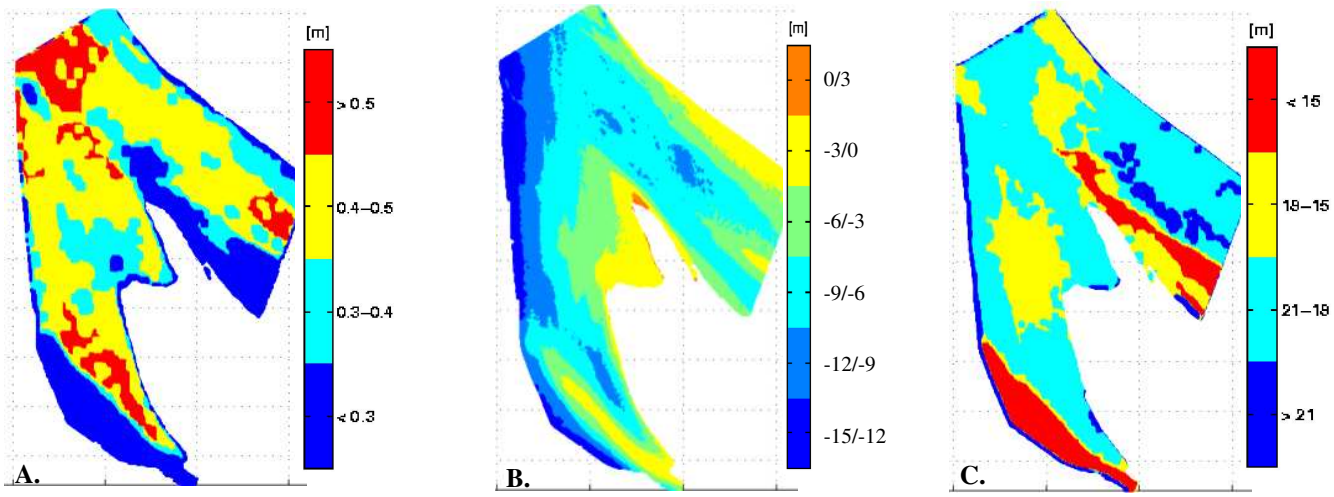

Fig. 4. Classification results. A. Sand dune amplitude, B. Depth, and C. Dune wavelength.

correlation can be found between depth on one hand and dune amplitude and wavelength on the other hand.

B. Sand dump area

In Fig. 1 the location of the sand dump is indicated. The sand is dumped after survey T0 and before survey T4, compare Table I. First the outline of the sand dump was reconstructed, then the redistribution of the deposited sand in the direct neighborhood of the dump location is determined. Because of the sand deposit, all bedforms were filled up. The recovery process of the sand dunes is monitored by determining the average sand dune wavelength and amplitude over the dump location as a function of time.

1) Dump erosion: In Fig. 5 the outline is drawn of the sand dump location as reconstructed from a deformation analysis of epochs T0-T4. Moreover, results of a deformation analysis over epochs T5-T16 are shown, giving insight in the dump erosion. On the bottom right, the most Northern point of the Plaat van Walsoorden is visible were echo sounding was not possible. Gray points were tested stable. At yellow to Red points, siltation occurred at an average rate of upto 1.5 cm a day corresponding to a total siltation of almost 2 m in 130 days. Erosion occurred for green to blue points of upto 2 cm a day. It can be seen that the dumped sand is moving South-East ward, in the direction of the Plaat van Walsoorden.

2) Sand dune recovery: The process of sand dune recovery is visualized in Fig. 6. As expected, the amplitude reaches a minimal value shortly after the finish of the deposit, around day 50. Then the amplitude gradually recovers until the original level of about 60 cm is reached again after 150 days.

TABLE II
CORRELATION COEFFICIENTS - AMPLITUDE, DEPTH, WAVELENGTH

	amplitude	depth	wavelength
amplitude	1	-.20	0.41
depth		1	-.06
wavelength			1

From this it is concluded that it takes almost four months for the subaqueous dunes to recover. The wavelength graph behaves different however. During and shortly after the sand dump, the wavelength is more or less stable according to the results of the profile line method. Then both methods indicate an increase in wavelength to a level of about 30 m. In this case the final parameter value after the sand dump is different from the value before. Possibly this is caused by the properties of the dumped sand. An explanation for the big peak in wavelength in the beginning for the variogram method can be found in Fig. 2. The experimental variogram of T3 displays almost no hole effect. Therefore the fitting of a hole effect model is not robust when the dune amplitude is low.

C. Stable area

A 'stable' area with uniform morphology parameter values in the North of the area of interest is selected based on the segmentation results, cf. Fig. 1. To asses the stability further,

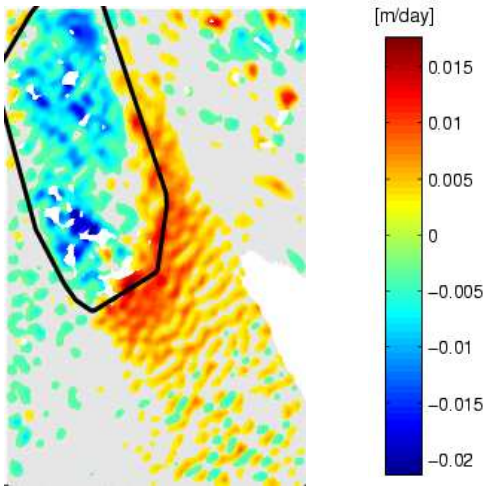

Fig. 5. Deformation of the sand dump.

a deformation analysis has been performed. This showed that on the eastern part of the initially selected 'stable' area deformation took place, possibly caused by sand dumping. This unstable part was therefore not considered in the further analysis. For the remaining grid points the average amplitude and wavelength is determined for all seventeen data epochs, using the methods as introduced in Section III-C. The results are shown in Fig. 7. The 'Profile' and 'Classification' methods, mentioned in the figure, are almost the same. In the first case profile directions are determined manually, in the second case automatically.

The results from the different methods are similar, only an offset occurs between the outcomes. These results show, that even for an area that is tested stable, the sand dune parameters slowly change over time. The amplitude drops more than 10 cm while the wavelength increases a few meter. A reason for this phenomenon is not yet known. No correlation could be detected with weather conditions in a first comparison for example. The jump after about 30 days may coincide with the sand dump: Possibly the quality of the soundings is affected by presence of loose sand in the water column over the sand dump area.

V. Conclusions

In this paper it is shown how to assess changes in depth and morphology in the complex topographic situation of a multichannel estuary. Different deformation regimes could be successfully distinguished by a combination of image analysis and statistical testing techniques. Although not shown here, it is possible to quantify the accuracy of the deformation analysis and the dune parameter value estimations.

A first attempt to link changes in parameter values to changing weather conditions was not successful, probably because no extreme weather events occurred in the period covered by the data.

Further research should focus on incorporating suited morphological attributes in the proposed analysis scheme, like bedform asymmetry, indicating dominant currents, local bedform orientation and local sediment properties.

VI. Acknowledgements

Special thanks go to the Flemish Authority, and especially to Ir. Yves Plancke for providing us with the MBES data of the Walsoorden experiment, thereby enabling this research.

References

[1] E. Leys, Y. Plancke, and S. Ides, "Shallow - Shallower - Shallowest, Morphological Monitoring Walsoorden," in *Proceedings Hydro'06, Evolutions in Hydrography*, Antwerp, Belgium, 2006.

[2] R. Lindenbergh, T. A. van Dijk, and P. J.P.Egberts, "Separating bedforms of different scales in echo sounding data waves and mega ripples." in *Proceedings Coastal Dynamics 2005*, Barcelona, Spain, 2006.

[3] P. J. G. Teunissen, *Adjustment theory*. Delft: Delft University Press, 2000.

[4] J. Winterwerp, Z. Wang, M. Stive, A. Arends, C. Jeuken, C. Kuijper, and P. Thoolen, "A new morphological schematization of the Western Scheldt estuary, the Netherlands," in *Proceedings 2nd IAHR Symposium on River, Coastal and Estuarine Morphodynamics*, Obihiro, Japan, 2001, pp. 525–534.

[5] C. Kuijper, R. Steijn, D. Roelvink, T. van der Kaaij, and P. Olijslagers, "Morphological modelling of the Western Scheldt: validation of DELFT3D," WL/Delft Hydraulics, Tech. Rep., 2004.

[6] D. van der Wal, P. M. Herman, and T. Ysebaert, "Space-borne Synthetic Aperture Radar of intertidal flat surfaces as a basis for predicting benthic macrofauna distribution," in *EARSeL eProceedings 3, 1/2004*, 2004.

[7] X. Lurton, *An Introduction to Underwater Acoustics*. Springer, 2002.

[8] F. Francken, S. Wartel, R. Parker, and E. Taverniers, "Factors influencing subaqueous dunes in the Scheldt Estuary," *Geo-Marine Letters*, vol. 24, no. 1, 2004.

[9] T. Lillesand and R. Kiefer, *Remote Sensing and Image Interpretation*, 4th ed. New York: Wiley, 2000.

[10] L. Dorst, "Survey plan improvement by detecting sea floor dynamics in archived echo sounder surveys," *International Hydrographic Review*, vol. 5, no. 2, pp. 49–63, 2004.

[11] P. Goovaerts, *Geostatistics for Natural Resources Evaluation*. New York, Oxford: Oxford University Press, 1997.

[12] J.-P. Chilès and P. Delfiner, *Geostatistics: modeling spatial uncertainty*, ser. Wiley Series in Probability and Statistics. New York: John Wiley & Sons, 1999.

[13] A. Jain, *Fundamentals of digital image processing*. Prentice-Hall, Inc., New Jersey, 1989.

[14] P. J. G. Teunissen, *Testing theory*. Delft: Delft University Press, 2000.

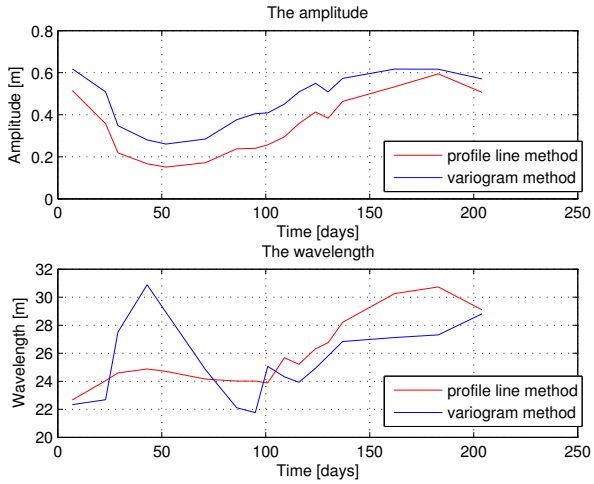

Fig. 6. Dune amplitude and wavelength at dump location over time.

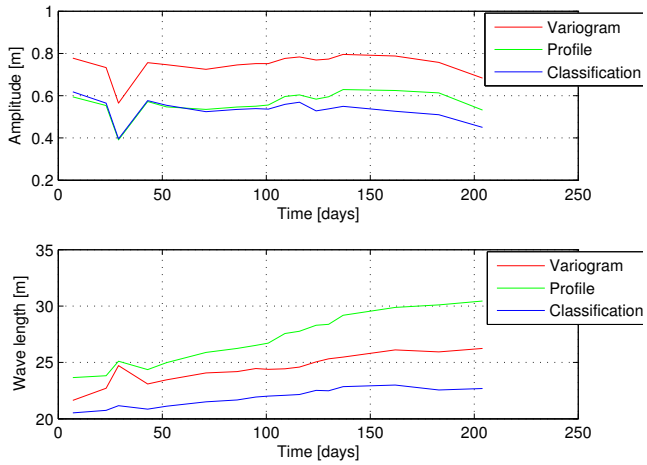

Fig. 7. Dune amplitude and wavelength at the 'stable' area over time.